

Harmonic Analysis and Performance Improvement of a Wind Energy Conversion System with Double Output Induction Generator

M. Sedighzadeh, and A. Rezazadeh

Abstract—Wind turbines with double output induction generators can operate at variable speed permitting conversion efficiency maximization over a wide range of wind velocities. This paper presents the performance analysis of a wind driven double output induction generator (DOIG) operating at varying shafts speed. A periodic transient state analysis of DOIG equipped with two converters is carried out using a hybrid induction machine model. This paper simulates the harmonic content of waveforms in various points of drive at different speeds, based on the hybrid model (dqabc). Then the sinusoidal and trapezoidal pulse-width-modulation control techniques are used in order to improve the power factor of the machine and to weaken the injected low order harmonics to the supply. Based on the frequency spectrum, total harmonics distortion, distortion factor and power factor. Finally advantages of sinusoidal and trapezoidal pulse width modulation techniques are compared.

Keywords—DOIG, Harmonic Analysis, Wind.

I. INTRODUCTION

IN order to maximize energy extraction from the wind, wind energy conversion systems (WECS) should be able to operate at variable rotational speed. Although variable speed operation demands higher complexity and initial investment, these drawbacks are offset by the increase of energy capture and the improvement of control flexibility [1]. Therefore, as wind technology progresses, an increasing number of variable speed WECS schemes are proposed.

An interesting configuration among them is the one that uses grid-connected double-output induction generator (DOIG) with slip energy recovery in rotor, shown in Fig. 1. At the cost of a wound rotor, DOIG provides several attractive features [2]. For instance: constant voltage and constant frequency generation (even operating at variable speed), generation above the machine rated power, and cheaper and smaller converter compared to those required for squirrel cage or synchronous generators (only slip power is processed). In addition, power control can be electronically implemented by modifying the DOIG torque through the firing angle of the converter.

The converter can be rated at a fraction of the generator rating for a limited speed range of applications. This leads to a lower cost of the power electronics components. Comparing

to ac part, ripple free dc link current, the most work based on dq model of the machine, simplifications are made on DOIG such as ignoring the injected harmonics to the system by rectifier/inverter, neglecting the overlap angle of the rectifier, larger time constant of dc part of rotor circuit compared with ac part, ripple free dc link current [3]. These simplifications for dc link current lead to an error in the predicted electromagnetic torque. The hybrid model (dqabc) keeps the real parameters of the rotor and takes into account the effect of the machine impedance on the overlap angle of rectifier, as well as simplifications for dc link current and rectifier/inverter harmonics, which are not made [4].

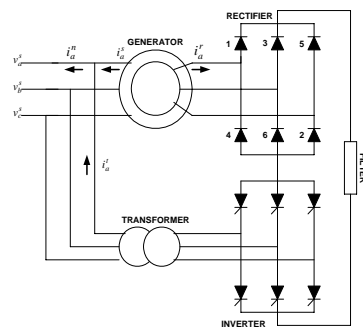


Fig. 1 Basic Power Circuit of a DOIG

The main drawback of static DOIG using cascade converters is its poor power factor. The reason is the reactive power absorbed by the generator, inverter and rectifier. By reducing the inverter reactive power absorbed by the inverter, power factor of the drive can be improved. One method for power factor improvement is the operation of inverter with a fly-wheeling control. For a three-phase inverter, a fly-wheeling control can be used with firing angles of between 90 and 120. For firing angles larger than 120, fly-wheeling control is not possible and power factor remains unchanged. The second method for power factor improvement is inverter operation with PWM technique. In this method, self-commutated switches (GTO or IGBT) replace the inverter thyristors and the inverter operates with a zero reactive power applying PWM technique [8].

II. SYSTEM MODELLING

The DOIG is simulated based on a hybrid model. This mathematical model consists of the models of induction generator, rectifier and inverter, as extensively described in [6].

Manuscript received January 5, 2008

The Authors are with Faculty of Electrical and Computer Engineering, Shahid Beheshti University, Tehran, 1983963113, Iran (phone: +98-21-29902290, fax: +98-21-22431804, e-mail: m_sedighi@sbu.ac.ir).

A. Phase-Controlled Inverter Model

The transformer and the main supply are assumed to have a negligible internal impedance. Consequently, the commutation overlap of the inverter can be neglected then inverter is modeled as a chopped sinusoidal voltage source with a period equal to one-sixth that of the supply. In this paper three phase controlled inverter model that its equations have been presented completely in [6,7] has been used.

B. PWM Controlled Inverter Model [9]

Normally commutated inverter in DOIG's demands some reactive power. In addition, it recovers active slip power to the supply. Consequently, the absorbed reactive power by whole system rises leading to a lower power factor of the drive. Also, a rather large low-order harmonics is injected to the supply.

The power factor of a converter can be improved using a forced commutation method. The amplitude of the harmonics can be also reduced. The PWM technique is one of the most effective methods in achieving the above goals. This method of improving the power factor eliminates the low-order harmonics.

However, the amplitude of the high-order harmonics is increased, which can be easily filtered. Various PWM techniques have been proposed [8].

To obtain a convenient performance, a current source type six valve converter from sinusoidal and trapezoidal pulse width modulation techniques controls with three-mode switching signals is used.

Here comparing sinusoidal and trapezoidal waveforms having a 120-phase difference and triangular carrier waveform, two-mode switching signals $x_i(t)(i=1,2,3)$ and three-mode switching signals are $x_i(t)$ obtained.

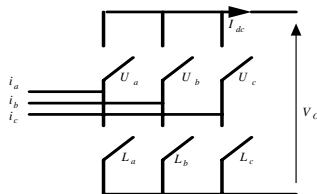


Fig. 2 Three-phase six-valve AC/DC inverter

TABLE I
TRANSFORMATION OF TWO AND THREE MODE SWITCHING

BI-LOGIC			THREE-LOGIC		
x_1	x_2	x_3	Y_a	Y_b	Y_c
+1	+1	+1	0	0	0
+1	+1	-1	0	+1	-1
+1	-1	+1	+1	-1	0
+1	-1	-1	+1	0	-1
-1	+1	+1	-1	0	+1
-1	+1	-1	-1	+1	0
-1	-1	+1	0	-1	+1
-1	-1	-1	0	0	0

Table I shows the validity of the transformation of two-mode switching to three-mode switching. The following linear relationship is used to obtain three-mode switching signals:

$$\begin{bmatrix} y_a(t) \\ y_b(t) \\ y_c(t) \end{bmatrix} = 0.5C \begin{bmatrix} x_1(t) \\ x_2(t) \\ x_3(t) \end{bmatrix}, \dots, C = \begin{bmatrix} 1 & \dots & -1 & \dots & 0 \\ -1 & \dots & 1 & \dots & -1 \\ -1 & \dots & 0 & \dots & 0 \end{bmatrix} \quad (1)$$

Fig. 2 presents a three phase six-valve ac/dc inverter. The following equations show the input currents, the output currents and the voltages of the converter:

$$I_K(t) = Y_K(t)I_{dc} \quad (2)$$

$$V_0 = \sum_K [Y_K(t)V_K], \dots, K = a, b, c \quad (3)$$

III. ANALYSIS OF THE SIMULATION RESULTS

A. Phase Control

In this study the firing angle of the inverter is taken to be 108 and the corresponding steady state speed 197.08 rad/s. Fig. 3(a) shows the rotor phase current waveform. The overlap caused by commutation impedance (stator, rotor and magnetizing impedances) leads to a non- rectangular current waveform. Fig. 3(a1) presents the harmonic spectrum of the rotor phase current. The use of the three phase rectifier bridge eliminates the third harmonic and its multiples. There are harmonics of the order $(6q \pm 1)$ where the signs+ and - express the positive and negative sequences. Fig. 3(b), (b1), (c), and (c1) show the rotor phase, line voltages and the corresponding frequency spectra respectively. The ripples on the rotor phase current and its large rate of variation result in pulsed voltage waveforms. As for the frequency spectrum, the harmonics of order $(6q \pm 1)$ appear in these voltages. The fundamental frequency of the rotor variables is s time the stator frequency $f_r = sf_s$. An ac/dc power converter causes the voltage and current harmonics in both ac and dc sides. In a six-pulsed converter, the harmonics on the dc side are $6q$ order and on ac side $6q \pm 1$ order [9]. Fig. 3(d) and (d1) show the dc link current and its frequency spectrum. Since this current is on the dc side of the two converters, from rectifier and inverter point of views, the diode bridge has $6qf_r$ harmonic components, both being on the same frequency spectrum. Fig. 3 (e), (e1), (f), and (f1) present secondary and primary currents and their corresponding frequency spectra. The drawbacks of injecting large low-order harmonics to the network and lower power factor can be attributed to these currents. Fig. 3 (g), (g1), (h), and (h1) present the stator phase current, the supply current and their corresponding frequency spectra respectively. The stator phase current is closer to a sinusoidal waveform (having less harmonics contents) compared with the rotor phase current, because the stator current is the sum of the generator magnetizing current and the rotor current phasors. The supply current is the summation the stator current and the reversed current of the transformer. The rectangular shape of the reversed current leads to a more distorted supply current compared with the stator current.

B. PWM Control

In this section the application of sinusoidal and trapezoidal PWM technique in DOIG for the power factor improvement of the supply, the reduction of the total reactive power consumption and the dc link ripples current and injected harmonics to the supply are shown. In the PWM technique, by changing the index modulation, the pulse width and the mean value of the inverter voltage are varied, thus the generator is controlled by the input voltage of the inverter (it depends on firing angle in phase control technique and modulation index in PWM technique). In order to compare the characteristics of the system in the three techniques, the mechanical torque and speed of the generator must be identical. Therefore, for modulation index 0.31 and $T_m = 20.N.m$ Nm, the speed of the generator is approximately 197.08 rad/s (in phase control technique it will be at $\alpha = 108$). The control system of the inverter has been designed based on the sinusoidal and trapezoidal PWM technique with three mode switching control. Fig. 4 and 5 (d,d1) show the simulated dc link current and its frequency spectrum respectively. The amplitude of the ripples of the dc link current oscillations is reduced while the oscillation frequency is increased and oscillation frequency resulting from the slip frequency of the rotor appears in it. The comparison of its frequency spectrum with the corresponding frequency spectrum from the phase control technique in Fig. 3(d1), indicates the reduction of the low-order frequency components. The rotor phase current and the rotor line voltage with their corresponding frequencies are shown in Fig. 4 and 5(a,a1,c,c1), respectively. The mean amplitude of these waveforms or the corresponding waveforms from the phase control technique is the same. So the amplitude and frequency of the ripple oscillations of the rotor current and the dc link current are identical. Rapid variations and almost linear ripples on the rotor current lead to pulses with the same frequency on the phase and line voltages. Table II compare THD due to the rotor current and voltage waveforms, the primary and secondary currents of the recovery transformer based on the control phase and PWM techniques. Considering these tables and the frequency spectra, THD of the phase current are almost identical while the harmonics contents (THD) of the rotor voltage has been decreased.

Fig. 4,5(f), (f1), (e), and (e1) show the primary and secondary of the recovery transformer currents and their frequency spectra, respectively. The largest effect of the PWM technique can be seen on these currents. Regarding these frequency spectra Fig. 4,5(e1) and the corresponding spectrum in Fig. 3(e1), the effective amplitude of the first harmonic and the low-order harmonics are largely weakened and transformed to the high-order harmonics. This is confirmed by comparing THD of these currents from Table II.

Fig. 4,5(h), (h1), (g), and (g1) show the stator phase and supply currents and their corresponding frequency spectra, respectively. The transforming the action of the rotor harmonics on the stator windings, the stator current contains speed-depending harmonics. Then the stator (and supply) current is no periodical. The equality of the harmonic contents of the rotor phase current using three controls techniques causes a similar harmonic distortion in the stator current. The comparison of Fig. 3(f1) and the corresponding frequency

spectrum well confirms the above result. The amplitude of the fundamental component and of every supply current harmonic are obtained from victories sum of the generator and inverter currents, as well as the supply harmonic currents are largely assigned to the inverter current, as the generator harmonic currents are relatively small. The harmonic contents and supply current are improved and low-harmonics eliminated due to the inverter effect if PWM technique is used. Table 3 shows the power factor of the DOIG when two different control techniques are used. Fig. 4 and 5(d,d1,e,e1) show the primary and secondary of the recovery transformer currents and their frequency spectra, respectively.

TABLE II
PERCENTAGE OF THD FOR DIFFERENT CONTROL TECHNIQUES

Control technique	Rotor phase current	Rotor phase voltage	Rotor line voltage	Transformer current secondary	Transformer current primary
Phase	18.07	16.33	16.52	29.06	26.34
Sinusoidal	17.67	14.07	14.26	27.67	23.67
Trapezoidal	16.82	13.05	13.95	27.24	20.98

TABLE III
POWER FACTOR FOR DIFFERENT CONTROL TECHNIQUES

Control technique	Power factor of the DOIG
Phase	0.56
Sinusoidal	0.65
Trapezoidal	0.71

IV. CONCLUSION

In this paper, the harmonic contents of various waveforms of the DOIG at different inverter techniques control have been shown using a detailed hybrid dqabc model. In this model, the actual rectifier overlap has been considered. The injected harmonics by the inverter/rectifier and ripples of the dc link current have been also taken into account. The presence of the recovery inverter using the phase control technique causes the injected low-order harmonics with rather large amplitude to the supply while the absorption of the reactive power can reduce the power factor. The application of the PWM control technique in the inverter with a forced commutation can improve the power factor of the drive and reduce the low-order harmonics injected to the supply; however amplitude of the high-order harmonics are increased which can be easily filtered.

REFERENCES

- [1] F. Giraud and Z. M. Salameh, "Wind-driven variable-speed, variable frequency, double-output, induction generators," *Electric Mach. Power Syst.*, vol. 26, pp. 287–297, 1998.
- [2] M. N. Eskander and M. T. El-Hagry, "Optimal performance of double output induction generator used in WECS," *Electric Mach. Power Syst.*, vol. 25, pp. 1035–1046, 1997.
- [3] E. Akpınar and P. Pillay, "Modeling and performance of slip energy recovery induction motor drives," *IEEE Trans. Energy Conversion*, vol. 5, pp. 203–210, Mar. 1990.
- [4] E. Akpınar and P. Pillay, "A computer program to predict the performance of slip energy recovery induction motor drives," *IEEE Trans. Energy Conversion*, vol. 5, pp. 357–365, June 1990.
- [5] J. B. Ekanayake, L. Holdsworth, X. Wu, N. Jenkins, "Dynamic Modelling of Doubly Fed Induction Generator Wind Turbines", *IEEE Trans. On power systems*, VOL.18, No. 2, May 2003, pp.803-809.

- [6] L. Refoufi, B. A. T. Alzahawi, A. G. Jack, "Analysis and modeling of the steady state behavior of the static Kramer induction generator," *IEEE Trans. On Energy Conversion*, Vol. 14, No. 3, September 1999, pp. 333-339.
- [7] Y. Baghouz and M. Azam, "Harmonic analysis of slip power recovery drives," *IEEE Trans. Ind. Applicat.*, vol. 28, pp. 50-56, Jan./Feb. 1992.
- [8] X. Wang and B. T. Ooi, "Unity power factor current source rectifier based on dynamic trilogic PWM," *IEEE Trans. Power Electron*, vol. 8, pp. 288-294, July 1993.
- [9] Jawad Faiz, H. Barati, and Eyup Akpinar, "Harmonic Analysis and Performance Improvement of Slip Energy Recovery Induction Motor Drives", *IEEE Trans. On Power Electronics*, Vol. 16, May. 2001, PP. 410-417.



M. Sedighzadeh received the B.S. degree in Electrical Engineering from the Shahid Chamran University of Ahvaz, Iran and M.S. and Ph.D. degrees in Electrical Engineering from the Iran University of Science and Technology, Tehran, Iran, in 1996, 1998 and 2004, respectively. From 2000 to 2007 he was with power system studies group of Moshanir Company, Tehran, Iran. Currently, he is an Assistant Professor in the Faculty of Electrical and Computer Engineering, Shahid Beheshti University, Tehran, Iran. His research interests are Power system control and modeling, FACTS devices and Distributed Generation.



A. Rezazade was born in Tehran, Iran in 1969. He received his B.Sc and M.Sc. degrees and Ph.D. from Tehran University in 1991, 1993, and 2000, respectively, all in electrical engineering. He has two years of research in Electrical Machines and Drives laboratory of Wuppertal University, Germany, with the DAAD scholarship during his Ph.D. and Since 2000 he was the head of CNC EDM Wirecut machine research and manufacturing center in Pishraneh company. His research interests include application of

computer controlled AC motors and EDM CNC machines and computer controlled switching power supplies. Dr. Rezazade currently is an assistant professor in the Power Engineering Faculty of Shahid Beheshti University. His research interests are Power system control and modeling, Industrial Control and Drives.

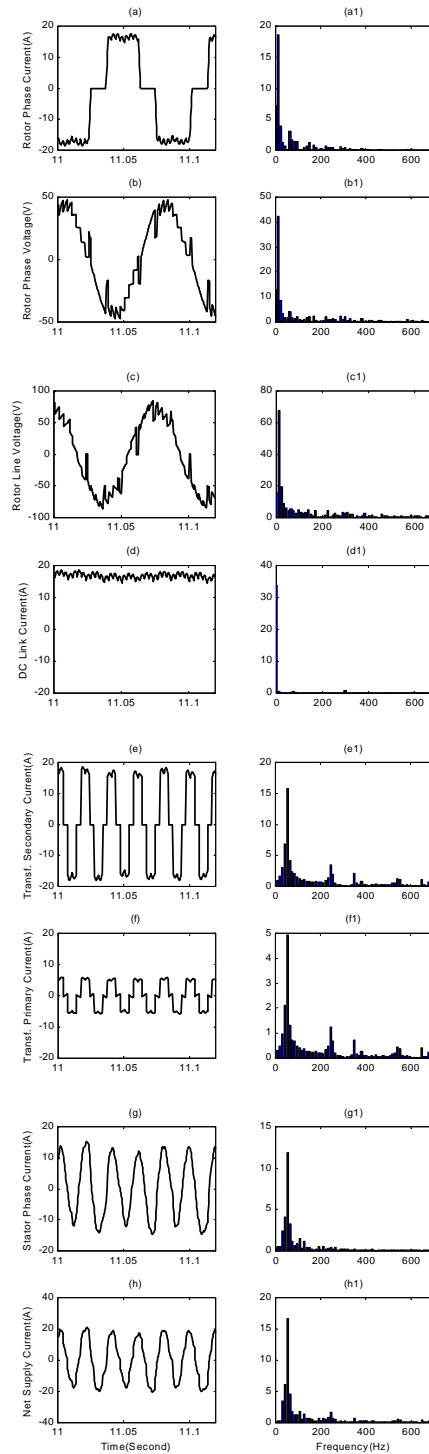


Fig. 3 Waveforms and harmonics content of: (a, a1) rotor phase current, (b, b1) rotor phase voltage, (c, c1) rotor line voltage, (d, d1) dc link current, (e, e1) transformer secondary current, (f, f1) transformer primary current, (g, g1) stator phase current, (h, h1) supply current.--(phase control)

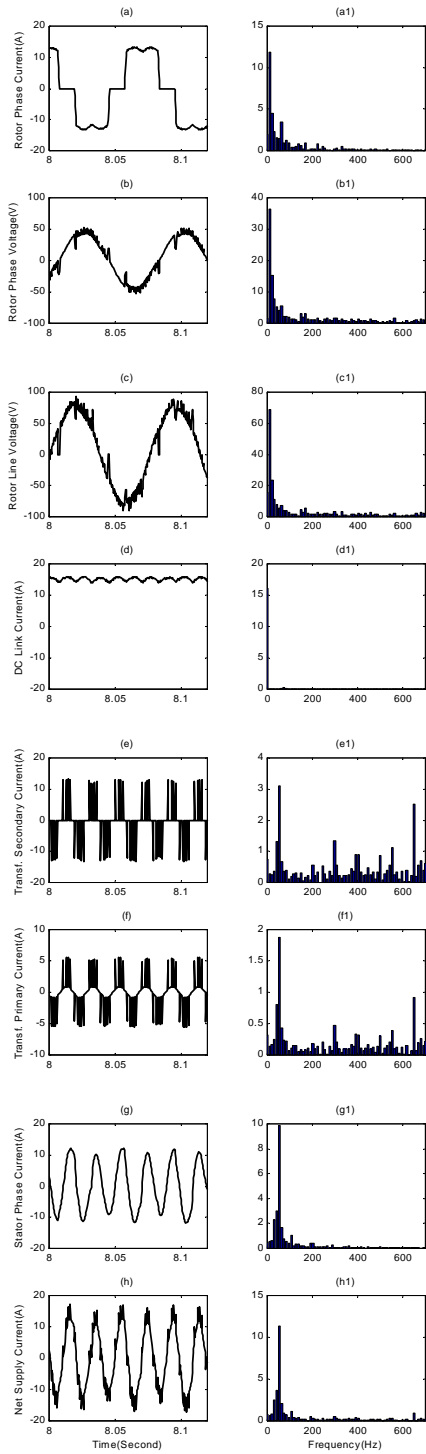


Fig. 4 Waveforms and harmonics content of: (a, a1) rotor phase current, (b, b1) rotor phase voltage, (c,c1) rotor line voltage, (d, d1) dc link current, (e, e1) transformer secondary current, (f, f1) transformer primary current, (g, g1) stator phase current, (h, h1) supply current.—(sinusoidal PWM control)

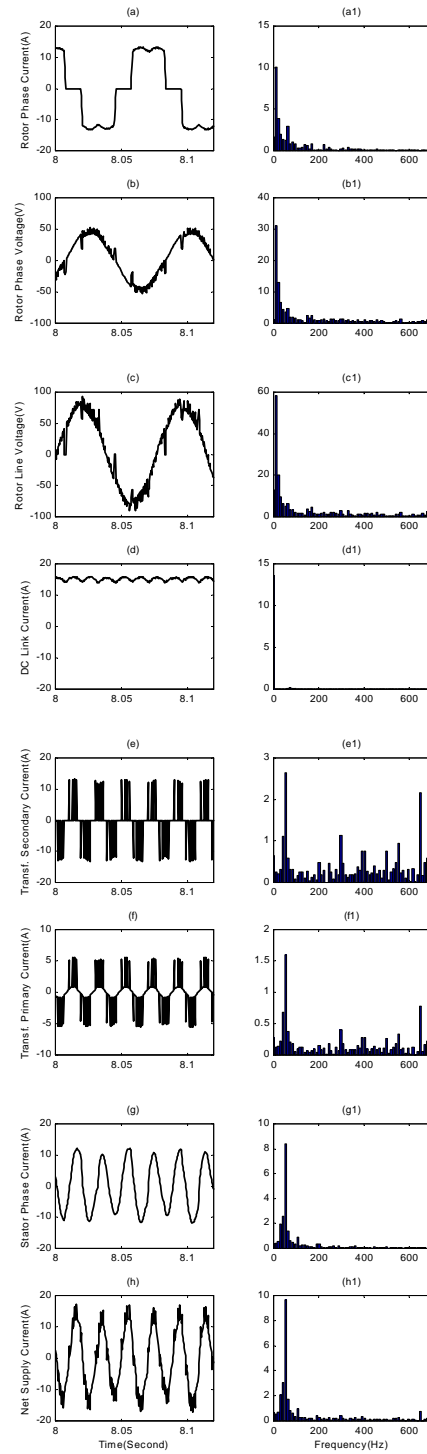


Fig. 5 Waveforms and harmonics content of: (a, a1) rotor phase current, (b, b1) rotor phase voltage, (c,c1) rotor line voltage, (d, d1) dc link current, (e, e1) transformer secondary current, (f, f1) transformer primary current, (g, g1) stator phase current, (h, h1) supply current.—(trapezoidal PWM control)